0026-895X/06/6902-440–451$20.00
MOLECULAR PHARMACOLOGY
Copyright © 2006 The American Society for Pharmacology and Experimental Therapeutics
Mol Pharmacol 69:440–451, 2006

Vol. 69, No. 2
15404/3078489
Printed in U.S.A.

Gene Transfer of Pro-opiomelanocortin Prohormone Suppressed the Growth and Metastasis of Melanoma: Involvement of α-Melanocyte-Stimulating Hormone-Mediated Inhibition of the Nuclear Factor κB/Cyclooxygenase-2 Pathway[S]

Guei-Sheung Liu, Li-Fen Liu, Che-Jen Lin, Jui-Cheng Tseng, Ming-Ju Chuang, Hing-Chung Lam, Jenn-Kuen Lee, Lin-Cheng Yang, Julie Hwa Yu Chan, Shen-Long Howng, and Ming-Hong Tai

Graduate Institute of Medicine, Kaohsiung Medical University, Kaohsiung, Taiwan (G.-S.L., S.-L.H., M.-H.T.); Department of Medical Education & Research (G.-S.L., C.-J.L., H.-C.L., J.H.Y.C., M.-H.T.), Division of Allergy, Immunology, and Rheumatology (J.-C.T.), and Division of Endocrinology and Metabolism, Department of Medicine (M.-J.C., H.-C.L., J.-K.L.), Kaohsiung Veterans General Hospital, Kaohsiung, Taiwan; Department of Biological Science and Technology (L.-F.L.) and Department of Anesthesiology, E-DA Hospital, I-Shou University (L.-C.Y.), Kaohsiung, Taiwan; and Department of Biological Sciences, National Sun Yat-Sen University, Kaohsiung, Taiwan (M.-H.T.)

Received June 14, 2005; accepted November 2, 2005

ABSTRACT

Pro-opiomelanocortin (POMC) is a prohormone of various neuropeptides, including corticotropin, α-melanocyte-stimulating hormone (α-MSH), and β-endorphin (β-EP). POMC neuropeptides are potent inflammation inhibitors and immunosuppressants and may exert opposite influences during tumorigenesis. However, the role of POMC expression in carcinogenesis remains elusive. We evaluated the antineoplastic potential of POMC gene delivery in a syngenic B16-F10 melanoma model. Adenovirus-mediated POMC gene delivery in B16-F10 cells increased the release of POMC neuropeptides in cultured media, which differentially regulated the secretion of pro- and anti-inflammatory cytokines in lymphocytes. POMC gene transfer significantly reduced the anchorage-independent growth of melanoma cells. Moreover, pre- or post-treatment with POMC gene delivery effectively retarded the melanoma growth in mice. Intravenous injection of POMC-transduced B16-F10 cells resulted in reduced foci formation in lung by 60 to 70% of control. The reduced metastasis of POMC-transduced B16-F10 cells could be attributed to their attenuated migratory and adhesive capabilities. POMC gene delivery reduced the cyclooxygenase-2 (COX-2) expression and prostaglandin (PG) E_2 synthesis in melanoma cells and tumor tissues. In addition, application of NS-398, a selective COX-2 inhibitor, mimicked the antineoplastic functions of POMC gene transfer in melanoma. The POMC-mediated COX-2 down-regulation was correlated with its inhibition of nuclear factor κB (NFκB) activities. Exogenous supply of α-MSH inhibited NFκB activities, whereas application of the α-MSH antagonist growth hormone-releasing peptide-6 (GHRP-6) abolished the POMC-induced inhibition of NFκB activities and melanoma growth in mice. In summary, POMC gene delivery suppresses melanoma via α-MSH-induced inhibition of NFκB/COX-2 pathway, thereby constituting a novel therapy for melanoma.

This work was supported in part by grants from the National Science Council, Taiwan (NSC 94-2752-B-075B-001-PAE, NSC 92-2320-B-075B-005 and NSC-93-2622-B-075B-001-CC3) and Kaohsiung Veterans General Hospital, Taiwan (VGHKS-92-30 and VGHKS-93-35).

Requests for research materials or reprints may be addressed to Dr. Shen-Long Howng, Department of Neurosurgery, Kaohsiung Medical University, 100 Shih-Chaun 1st Road, Kaohsiung 80708, Taiwan. E-mail: shloho@ms.kmuh.org.tw

[S] The online version of this article (available at http://molpharm.aspetjournals.org) contains supplemental material.

Article, publication date, and citation information can be found at http://molpharm.aspetjournals.org.
doi:10.1124/mol.105.015404.

POMC is a multifunctional polycistronic gene located on human chromosome 2p23.3. POMC is a 31 kDa prohormone that is processed into various neuropeptides, including corticotropin, melanotropins (α-, β-, and γ-MSH), lipotropins, and β-endorphin (β-EP) (Solomon, 1999; Catania et al., 2004b). POMC peptides possess pleiotropic functions including pigmentation, adrenocortical function, regulation of energy stores, the immune system, and the central and peripheral

ABBREVIATIONS: POMC, pro-opiomelanocortin; β-EP, β-endorphin; α-MSH, α-melanocyte-stimulating hormone; MC1R, melanocortin 1 receptor; GHRP-6, growth hormone-releasing peptide-6; NS-398, *N*-[2-(cyclohexyloxyl)-4-nitrophenyl]-methane sulfonamide; m.o.i., multiplicity of infection; H-89, *N*-[2-(4-bromocinnamylamino)ethyl]-5-isoquinoline; PCR, polymerase chain reaction; RIA, radioimmunoassay; PBMC, peripheral blood mononuclear cell; ELISA, enzyme-linked immunosorbent assay; MTT, 3-(4,5-dimethylthiazol-2-yl)-2,5-diphenyltetrazolium; GFP, green fluorescent protein; PBS, phosphate-buffered saline; pfu, plaque-forming units; RT, reverse transcription; PCR, polymerase chain reaction; HRP, horseradish peroxidase; IL, interleukin; IFN, interferon; PKA, protein kinase A; COX, cyclooxygenase.

nerve systems (Catania et al., 2004b). POMC expression in the hypothalamus or brainstem gives rise to melanocortinergic neurotransmitters, whereas expression in the pituitary gland gives rise to circulating melanocortin hormones (Raffin-Sanson et al., 2003). The specific patterns of post-translational POMC processing dictate whether an individual cell releases α-MSH, corticotropin, or other melanocortin peptides, which in turn control overlapping arrays of endocrine and metabolic and neurologic endpoints.

POMC processing was believed to occur primarily in the pituitary gland and the central nervous system. POMC neuropeptides such as α-MSH and β-EP have been identified in various non-neuronal cells, including memory T cells, macrophages, and melanocytes (Schauer et al., 1994; Cabot et al., 1997; Raffin-Sanson et al., 2003). In addition, *POMC* gene delivery in muscle or bladder by gene gun approach alleviates pain via local generation of β-EP (Lu et al., 2002; Chuang et al., 2003), indicating that POMC could be processed in the peripheral tissues to elicit antinociceptive effect.

The anti-inflammatory and immunosuppressive functions of POMC neuropeptides have been characterized (Luger et al., 2003; Catania et al., 2004b). POMC neuropeptides, particularly corticotropin and α-MSH, are potent inhibitors of inflammation. Corticotropin stimulates the adrenal gland to release cortisol, which exerts anti-inflammatory functions directly or via the synthesis of glucocorticoid. The anti-inflammatory nature of α-MSH has been proposed for the treatment of various inflammation-related diseases (Catania et al., 1999, 2004b). The immune-modulating functions of POMC neuropeptides have been elucidated (Luger et al., 2003). Corticotropin and its downstream products, cortisol and glucocorticoid, are potent immunosuppressive agents. α-MSH regulates the immune responses by impairing the functions of both antigen-presenting cells and T cells (Luger et al., 1998) and by modulating the production of pro-inflammatory and anti-inflammatory cytokines (Luger et al., 2003). β-EP inhibits the immune system at multiple levels such that elevated splenocyte proliferation and cytokine production were observed in β-EP-deficient mice (Refojo et al., 2002).

The influence of POMC expression during tumor progression remains elusive. POMC expression is repressed in tumor tissues because of promoter methylation (Newell-Price et al., 2001). In malignant mesothelioma cells, expression of POMC transcripts, POMC-processing enzymes, and melanocortin 1 receptor (MC1R), the high-affinity receptor for α-MSH, constitutes an autocrine-inhibitory circuit to suppress the proliferation of tumor cells (Catania et al., 2004a). Furthermore, α-MSH inhibits the production of prostaglandins (Nicolaou et al., 2004) and contributes to the prevention of melanoma by reduction of UV-induced DNA damage in melanocytes (Kadekaro et al., 2003). These findings supported the idea that POMC overexpression might inhibit inflammatory responses to intervene tumor progression (Manna and Aggarwal, 1998; Coussens and Werb, 2002). However, based on the concept of immunosurveillance against cancer development, POMC expression could result in dysfunction of host immune system, thereby allowing tumor cells to escape from immune scrutiny. Because elevated plasma α-MSH levels was found to correlate with malignancy in patients with melanoma (Ghanem et al., 1989; Liu and Johansson, 1995), the correlation between α-MSH levels and melanoma progression implicated that POMC expression might modulate the immune response and create favorable environment for tumor invasion. Therefore, whether POMC expression promoted or suppressed tumor progression remains controversial. In the present study, we investigated the outcome of *POMC* gene delivery on growth and metastasis of melanoma using syngenic B16-F10 melanoma model, thereby delineating the interplay between anti-inflammatory and immunosuppressive functions by *POMC* overexpression.

Materials and Methods

Cell Cultures and Reagents. For production and propagation of Ad5 adenovirus, E1a-transformed human embryonic kidney 293 cells were purchased from Microbix Biosystems Inc. (Toronto, ON, Canada) and maintained at low passage. B16-F10 melanoma cells were purchased from the American Type Culture Collection (Manassas, VA) and cultured in Dulbecco's modified Eagle's medium (Invitrogen, Carlsbad, CA) containing 10% fetal calf serum, 2 mM glutamine, 100 mg/ml streptomycin, and 100 U/ml penicillin at 37°C in a 5% CO_2 incubator. Corticotropin, α-MSH, β-EP, and GHRP-6 were purchased from Bachem California (Torrance, CA). NS-398 was from Cayman Chemical Co. (Ann Arbor, MI). Naloxone, H-89, and concanavalin A were from Sigma (St. Louis, MO)

Generation of Recombinant Ad-POMC. Human POMC cDNA (Lin et al., 2002) was subcloned into KpnI site of adenovirus transfer vector Ad5–2 to yield Ad5–2-POMC, in which the transgene was driven by long terminal repeat promoter from the Rous sarcoma virus and flanked by polyadenylation sequences from bovine growth hormone. Recombinant adenovirus was generated by cotransfection of pAd5–2-POMC with pJM17 vector (Microbix), a plasmid containing the entire type 5 Ad genome with E1-insertion and E3-deletion, into 293 cells as described previously (Tai et al., 2003). After homologous recombination, the virus plaques were verified by checking for cytopathic effect and PCR. The virus was amplified by two rounds of cesium chloride ultracentrifugation and desalted by G-25 gel-filtration chromatography. The titer of virus solution was determined by measuring optical density at 260 nm and plaque-forming assay on 293 cells before storage at −80°C.

Radioimmunoassays. Corticotropin and β-EP concentrations were determined using RIA kits (Nichols Institute Diagnostics, San Juan Capistrano, CA) with a linear range of measurement between 5 and 1000 pg/ml for corticotropin or β-EP and a detection threshold of 5 pg/ml. α-MSH RIA kit (Euro-Diagnostica, Malmö, Sweden) was used for measurement of α-MSH. The detection limit of this assay was 5 pg/ml with no cross-reactivity. A standard curve was constructed for each assay. Experiments were performed at least three times.

Melanin Assay. The melanin production in the cultured media of B16-F10 cells was determined by measurement of the absorbance at the wavelength of 475 nm and the cultured media from untreated cells was used as blank. The melanin content in cell culture was normalized with the cell number.

Isolation and Stimulation of Peripheral Blood Mononuclear Cells. PBMCs were prepared from heparinized whole blood using Ficoll-Hypaque (GE Healthcare, Little Chalfont, Buckinghamshire, UK) gradient centrifugation. The blood samples were diluted 1:1 with sterile PBS and carefully layered over Ficoll-Hypaque followed by centrifugation at 1800 rpm at 4°C for 20 min. The interface containing PBMC was harvested and washed twice with ice-cold, serum-free RPMI 1640 medium (Invitrogen). After resuspension in RPMI 1640 medium containing 10% fetal calf serum, 100 U/ml penicillin, 100 μg/ml streptomycin, and 2 mM L-glutamine, the viability of PBMC was analyzed by trypan blue exclusion assay. In the presence of concanavalin A (25 μg/ml), PBMC (1×10^6 cells per well in a six-well plate) in 1 ml of cultured media were incubated with

equal volume of conditioned media from infected B16-F10 cells at 37°C for 24 h. Thereafter, cultured media of stimulated PBMC was harvested for cytokine determination.

Enzyme-Linked Immunosorbent Assay. The concentrations of IL-2, interferon γ (IFN-γ), and IL-10 in cultured media of PBMC were measured by their specific ELISA kits (R&D Systems Inc., Minneapolis, MN) following protocols provided by manufacturer. The release of PGE_2 in cultured media was determined by the PGE_2 enzyme immunoassay kit (Cayman Chemical) following the manufacturer's protocol.

Cell Proliferation Assay. B16-F10 cells were cultured in a 96-well plate at a density of 4×10^4 cells/ml. After infection with adenovirus vectors, cells were supplemented with fresh medium containing 3-(4,5-dimethylthiazol-2-yl)-2,5-diphenyltetrazolium bromide (MTT; 0.456 mg/ml) and incubated for 1 to 2 h at 37°C. The formazan in viable cells was dissolved with 100 μl of dimethyl sulfoxide and determined by reading optical densities in a microplate reader (Dynex Technologies, Inc., Chantilly, VA) at an absorption wavelength of 570 nm.

Soft Agar Assay. After infection for 12 h, B16-F10 cells (5×10^3 cells) were seeded in 0.3% agarose (Difco, Detroit, MI) containing growth medium and added onto 6-cm plate prelayered with 0.5% bottom agarose (Difco) containing growth medium. The plates were incubated at 37°C and 5% CO_2 for 1 to 2 weeks until colonies developed. The number of colonies (>50 cells per colony) in each well was scored.

GFP-Expressing Melanoma Cells and GFP Fluorescence Assays. pEGFP-C1 plasmid (Clontech, Mountain View, CA) was transfected into B16-F10 cells by Lipofectamine (Invitrogen). The GFP-expressing clones were obtained by G418 selection and verified using Western blotting and fluorescence microscope analysis. The tissue extracts were isolated using lysis buffer containing 150 mM NaCl, 50 mM Tris-HCl pH 7.8, 1% Nonidet P-40, and complete protease inhibitors (Roche Applied Science, Indianapolis, IN). After extraction, the GFP fluorescence intensity was determined in a fluorometer (FLUOstar; BMG LABTECH GmbH, Offenburg, Germany).

Primary and Metastatic Melanoma Models. Animal experiments were carried out in Animal Center of Kaohsiung Veterans General Hospital in accordance with institutional guidelines. Male C57BL/6 mice (6–8 weeks old; The Animal Center of National Science Council; Taipei, Taiwan) were acclimated and caged in groups of four or less. All mice were fed with a diet of animal chow and water ad libitum. Animals were anesthetized in a methoxyflurane chamber before all procedures and sacrificed by a lethal dose of methoxyflurane.

In the chemoprevention or pretreatment paradigm, B16-F10 cells were infected with adenovirus vectors for 12 h, then subcutaneously injected into C57BL/6 mice (5×10^5 cells in 0.1 ml of PBS per mice) to monitor tumor growth. To evaluate the therapeutic potential of *POMC* gene delivery, melanoma were grown in mice to the size of at least 100 mm^3 and then administrated with adenovirus vectors (1×10^9 pfu) in 100 μl of PBS by intratumor injection. NS-398 was administered into mice via intraperitoneal route daily at a dose of 10 mg/kg as described previously (Duff et al., 2003). Tumor volumes were measured with a dial caliper and determined using the formula: volume = $\text{width}^2 \times \text{length} \times 0.52$.

In the pulmonary metastasis model, mice were divided into three groups [1) untreated, 2) Ad-POMC-infected cells, or 3) Ad-GFP-infected B16-F10 cells (5×10^5 cells in 200 μl of PBS per mouse)]. Cells were administered via tail vein to induce metastatic melanoma in lung. The metastasis to lung was detected at day 14 after injection.

Cell Adhesion Assay. The adhesion assay was performed as described previously (Zhong Wu et al., 2004). Laminin or fibronectin (both from Roche Applied Science) was dissolved in PBS to a final concentration of 50 μg/ml and used for coating by adding 0.1 ml of solution per well in a 96-well plate at 4°C overnight. All groups were assayed at the same time in quadruplicate. After overnight incubation, the wells were washed with PBS twice and incubated with serum-free Dulbecco's modified Eagle's medium at 37°C for 30 min. Cells (2×10^4) were added to each well and incubated at 37°C from 30 min to 4 h for adhesion. After incubation, the adhered cells were gently washed twice with PBS and measured using MTT assay.

Scratch Migration Assay. The migration of melanoma cells was assessed using a scratch migration assay as described previously (Zhu et al., 2004). In brief, after infection with adenovirus vectors for 12 h, a gap of approximately 1 mm was created in the adherent layer of confluent B16-F10 cells (in six-well plates) by introducing a scratch using a sterile 0.1-ml pipette tip (Gilson, Inc., Middleton, WI). The closure extent of the cell-free gap was recorded by microscopy at different time intervals and counted over a period of 24 h.

Quantitative Real-Time RT-PCR. RNA was isolated from cells using RNAzol (Tel-Test Inc., Friendswoods, TX). For reverse transcription, 5 μg of total RNA was used for reverse transcription with Superscriptase II (Invitrogen) using oligo-dT and random primers. One twentieth of reverse-transcription products were used as template for quantitative real-time RT-PCR in a Prism 7700 sequence detector (Applied Biosystems, Foster City, CA) using a SYBR green assay. PCR reaction was performed in 50 μl of SYBR Green PCR Master Mix (Applied Biosystems) containing 10 μM forward and reverse primers and approximately 30 ng of cDNA. Amplification and detection were performed: one cycle of 95°C for 10 min and 40 cycles of 95°C for 15 s, 62°C for 20 s, and 72°C for 15 s. After completion, a final melting curve was performed by denaturation at 95°C for 15 s and then was recorded by cooling to 60°C and then heating slowly until 95°C for 20 min according to the dissociation protocol of ABI 7700 instrument. The primer sequences for COX-2 (forward primer, 5′-GGTGTATCCCCCCACAGTCA-3′; reverse primer, 5′-CCAGGCACCAGACCAAAGAC-3′) amplified a 110-base pair COX-2 cDNA fragment. The β-actin mRNA level was determined using a forward primer (5′-TCACCCACACTGTGCCCATCTACGA-3′) and reverse primer (5′-CAGCGGAAC CGCTCATTGCCAATGG-3′) that amplified a 295-base pair β-actin cDNA fragment.

Western Blot Analysis. B16-F10 cells were infected with adenovirus vectors at multiplicities of infection (m.o.i.) of 500 or 1000. After 12 h, cells were supplemented with fresh medium and continued to incubate at 37°C for an additional 48 h. The protein extract was isolated using buffer containing 150 mM NaCl, 50 mM HEPES, pH 7, 1% Triton X-100, 10% glycerol, 1.5 mM $MgCl_2$, 1 mM EGTA, and protease inhibitors (Roche Applied Science). After separation in 12.5% SDS-PAGE, proteins were transferred onto polyvinylidene fluoride membranes using blotting apparatus. The membrane was blocked with 5% milk in Tris-buffered saline/Tween 20 for 1 h then incubated with NFκB (1:500 dilutions) or COX-2 antibodies (1:500 dilutions; both from Santa Cruz Biotechnology, Santa Cruz, CA) for 1 h at room temperature. After secondary antibody was conjugated with HRP (1:5000 dilutions in 5% milk) for 30 min, the signals on membrane were detected using ECL Plus luminol solution (GE Healthcare) and expose to X-ray film for autoradiography.

Immunohistochemistry. The paraffin-embedded melanoma tissue blocks were sectioned into 3-μm slices and mounted on poly(L-lysine)-coated slides. After deparaffinization, the slides were blocked with 3% hydrogen peroxide for 10 min and subjected to antigen retrieval with microwave in 10 mM citrate buffer for 15 min. The slides were incubated with COX-2 antibodies (1:200 dilution; Cayman) at 4°C overnight. After wash with PBS, the sections were incubated with horseradish peroxidase/Fab polymer conjugate (polymer detection system; Zymed Laboratories, South San Francisco, CA) for 30 min and detected using diaminobenzidine (1:20 dilution; Zymed Laboratories).

NFκB Activity Assay. The NFκB activities in melanoma cells were investigated by luciferase activities assay and electrophoretic mobility shift assay. For luciferase assay, B16-F10 cells (in a six-well plate) at 80% confluence were cotransfected with NFκB-driven luciferase (Stratagene, La Jolla, CA) vector and the *Renilla reniformis* luciferase reporter vector (Promega, Madison, WI) at a ratio of 1:1/10

using Lipofectamine (Invitrogen). After subsequent infection with adenovirus vectors, the NFκB-driven luciferase activities in cells were determined using a Dual-Light kit (Promega, Madison, WI) in a luminometer (Microlumat Plus LB96V; Berthold Technologies, Bad Wildbad, Germany) and normalized with that of *R. reniformis* luciferase according to manufacturer's instructions.

For electrophoretic mobility shift assay, the double-stranded oligonucleotides for the consensus binding sites of NFκB (5′-AGTTGAGGGGACTTTCCCAGGC-3′) were labeled using Klenow fragment (Invitrogen) in the presence of 100 μCi of [α-^{32}P]dCTP (3000 Ci/mmol; PerkinElmer Life and Analytical Sciences, Boston, MA) and unlabeled dATP, dGTP, and dTTP at 100 μM in a final volume of 50 μl. The unincorporated nucleotides were removed using a G-25 spin column (GE Healthcare). Five micrograms of nuclear proteins were incubated with reaction buffer [50 μg/ml poly(dI-dC), 5% glycerol, 10 mM Tris-HCl, pH 7.8, 1 mM EDTA, 40 mM KCl, and 1 mM dithiothreitol] on ice for 20 min before addition of the radiolabeled oligonucleotide probe for an additional 20 min at room temperature. The reaction products were separated in a 4% polyacrylamide gel. Gels were run at room temperature at 10 V/cm for 45 min, dried in a gel dryer under vacuum at 80°C, and analyzed by autoradiography.

Statistical Analysis. Differences between the groups were statistically evaluated using the unpaired Student's *t* test. The results are presented as mean ± S.D. All *P* values were two-tailed, and a *P* value of less than 0.05 was considered statistically significant.

Results

Adenovirus-Mediated POMC Overexpression in B16-F10 Melanoma Cells Increased the Production of Immunomodulatory POMC Neuropeptides. The E1-, E3-defective recombinant adenovirus encoding POMC (Ad-POMC) was generated for gene delivery studies. By infection with adenovirus encoding green fluorescent protein (Ad-GFP) at various multiplicities of infection, the optimal condition for adenovirus vectors to infect B16-F10 melanoma cells was determined at a m.o.i. of 500 or 1000 (Supplemental Data). Under these conditions, most B16-F10 melanoma cells expressed GFP without overt cytotoxicity. To evaluate the efficacy of POMC processing, the levels of POMC neuropeptides in the cultured media of B16-F10 cells were determined by RIAs. Ad-POMC-infected B16-F10 cells released significantly higher levels of corticotropin, β-EP, and α-MSH compared with cells of control groups ($P < 0.001$; Fig. 1a).

Because α-MSH stimulates melanogenesis in melanocytes, we examined the morphologies and melanin secretion in POMC-transduced melanoma cells. Indeed, Ad-POMC-infected B16-F10 cells exhibited characteristic features of melanogenesis including a significantly higher melanin release and dendritic phenotype with increased dark deposits (Supplemental Data). Thus, *POMC* gene delivery increases the production of bioactive POMC neuropeptides, such as α-MSH, in melanoma cells.

To investigate the immunomodulatory influence of POMC neuropeptides produced by melanoma cells, the cytokines release from PBMCs was evaluated after incubation with cultured media from POMC-transduced melanoma cells. Treatment with cultured media of POMC-transduced cells significantly attenuated the release of anti-inflammatory cytokines such as interleukin-2 and IFN-γ in PBMC (Fig. 1b). On the contrary, incubation with cultured media of POMC-transduced cells significantly increased the production of anti-inflammatory interleukin-10 (IL-10) in PBMC. Together, these results validate that POMC gene transfer in melanoma cells leads to enhanced secretion of POMC neuropeptides, which differentially regulate the expression of pro- and anti-inflammatory cytokines in lymphocytes.

POMC Gene Transfer Inhibited the Growth of Melanoma in Vitro and in Vivo. To evaluate the antitumor effect of *POMC* gene delivery, the proliferation and colony-

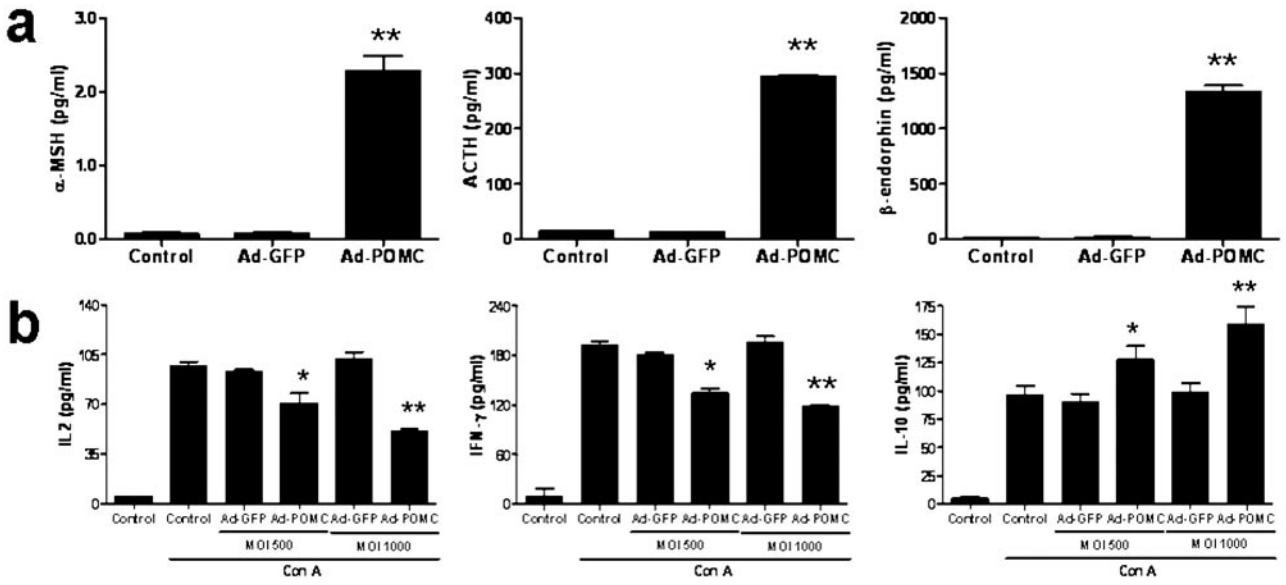

Fig. 1. The immunomodulatory effect of POMC neuropeptides in B16-F10 cells after POMC gene delivery. a, effect of *POMC* gene delivery on the levels of corticotropin, α-MSH, and β-EP in conditioned medium of B16-F10 cells. After infection with adenovirus vectors for 48 h, conditioned medium were harvested from B16-F10 cells and analyzed for the levels of POMC-derived peptides [corticotropin (ACTH), α-MSH, and β-EP] by RIA. There was a significant difference between control and Ad-POMC-treated groups. **, $P < 0.001$. b, effect of conditioned media from POMC-transduced B16-F10 cells on inflammation-related cytokines expression in PBMCs. After incubation of PBMC with conditioned media from various adenovirus-infected B16-F10 cells for 24 h in the absence or presence of concanavalin A (Con A; 25 μg/ml), the secretion level of IL-2, IFN-γ, and IL-10 in stimulated PBMC was determined by ELISA. The results were expressed as mean ± S.D. of triplicate experiments. There was a significant difference between control and Ad-POMC-treated groups. *, $P < 0.05$; **, $P < 0.01$.

forming capability of B16-F10 cells were investigated after POMC gene delivery. Despite marginal inhibition of cell proliferation (Fig. 2a), POMC gene transfer prominently inhibited the anchorage-independent growth of B16-F10 cells in soft agar by more than 50% of control groups (Fig. 2b). To further explore the antineoplastic potential of POMC gene delivery in vivo, B16-F10 cells were pretreated by infection with adenovirus vectors then injected subcutaneously into C57BL/6 mice to induce melanoma (Fig. 2c). The tumor size in mice implanted with POMC-transduced B16-F10 cells was significantly retarded (1625 ± 305 mm^3 at day 19) compared with mice implanted with cells of control groups (3098 ± 525 and 2866 ± 559 mm^3 for PBS- and Ad-GFP-treated B16-F10 cells, respectively, at day 19; $P < 0.01$). Moreover, in mice with established melanoma, post-treatment by administration of Ad-POMC, but not Ad-GFP or PBS, potently inhibited the progression of melanoma (tumor size in Ad-POMC-, PBS-, or Ad-GFP-treated mice was 1420 ± 145, 4512 ± 548, or 4286 ± 259 mm^3, respectively, at day 21; $P < 0.01$; Fig. 2d). These results indicate that POMC gene transfer effectively suppresses the tumorigenicity of primary melanoma.

***POMC* Gene Transfer Perturbed the Lung Metastasis of Melanoma Cells.** To investigate the effect of POMC gene transfer on the metastatic potential of melanoma cells, GFP-expressing B16-F10 cells (GFP-B16-F10 cells) were generated for tracking metastatic melanoma cells (Fig. 3a). Intravenous injection of GFP-B16-F10 cells resulted in formation of numerous metastatic foci in lung within 14 days. The events of lung metastasis could be quantified by measuring either the foci number or GFP fluorescence intensity in lung (Fig. 3b). After infection with adenovirus vectors, the transduced GFP-B16-F10 cells were intravenously injected into mice at day 0, and the formation of pulmonary colonies was evaluated on day 14. The number of metastatic foci in mice injected with Ad-POMC-treated GFP-B16-F10 cells (6.05 ± 4.47 foci per lung) was significantly lower than that of control groups (17.4 ± 4.38 and 24.4 ± 5.78 foci per lung for Ad-GFP- and PBS-treated groups, respectively; $P < 0.01$; Fig. 3, c and d). Besides, quantification of GFP fluorescence in lung tissues revealed that GFP expression lung tissues from mice injected with Ad-POMC-infected cells was significantly decreased compared with control groups (Fig. 3e). Together, these results suggest that POMC gene delivery attenuates the metastatic potential of B16-F10 cells in vivo.

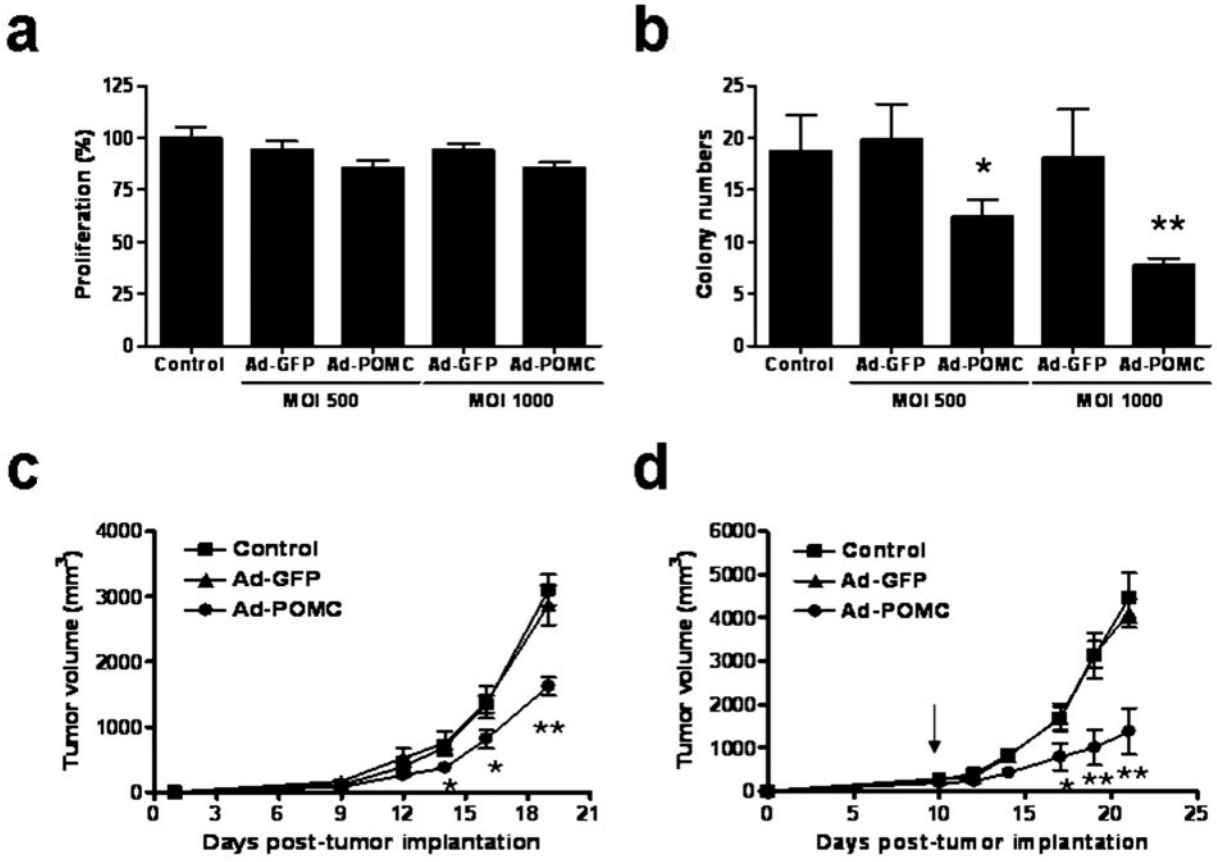

Fig. 2. Effect of *POMC* gene delivery on the tumorigenesis of B16-F10 melanoma cells. a, effect of *POMC* gene delivery on proliferation of B16-F10 melanoma cells. After infection with adenovirus vectors for 48 h, the proliferation of B16-F10 melanoma cells was determined by MTT assay and expressed as mean percentage of control ± S.D. from quadruplicate experiments. b, effect of *POMC* gene delivery on anchorage-independent growth of B16-F10 melanoma cells in soft agar. After 14 days in soft agar, the number of colonies in different groups of B16-F10 melanoma cells were scored and expressed as mean percentage of control ± S.D. from triplicate experiments. c, tumor growth in mice after implantation of POMC-transduced B16-F10 melanoma cells. B16-F10 cells were infected with adenovirus vectors at an m.o.i. of 1000 for 12 h then implanted into C57BL/6 mice at day 0. The tumor volumes in mice were measured at different time intervals. The results were representative of three independent experiments. *, $P < 0.05$; **, $P < 0.01$. d, effect of POMC gene delivery on established melanoma in mice. Mice were implanted with B16-F10 melanoma cells at day 0. After tumor size in each mouse was at least 100 mm^3 at day 10, mice were randomly divided into three groups ($n = 8$) and treated with Ad-GFP (1×10^9 pfu), Ad-POMC (1×10^9 pfu), or PBS by intratumor injection. Arrow indicates the date of injection. The results were representative of three independent experiments. **, $P < 0.01$.

***POMC* Gene Transfer Attenuated the Motility and Adhesion of Melanoma Cells to Extracellular Matrix.** To investigate the mechanism underlying attenuated metastasis by POMC gene delivery, the migration of infected B16-F10 cells was investigated by a scratch wound assay (Fig. 4a). The gap area in PBS- or Ad-GFP-treated cells was completely healed within 24 h, whereas the gap in Ad-POMC-infected cells was not filled up in the same time interval. Quantitative analysis of wound area revealed a significant reduction of wound closure in Ad-POMC-infected cells compared with cells of control groups at 24 h ($P < 0.01$; Fig. 4a). These data suggest that *POMC* gene delivery reduces the motility of melanoma cells.

Because the attachment to extracellular matrix is pivotal to the colonization of metastatic cells in distant organs, we examined the influences of *POMC* gene transfer on the adhesion properties of melanoma cells to extracellular matrix proteins. Despite moderate effects in binding caused by viral infection, *POMC* gene transfer caused significantly reduced binding affinity in B16-F10 cells to fibronectin ($P < 0.05$; Fig. 4b) or laminin ($P < 0.05$; Fig. 4c). Together, these findings indicate that POMC-mediated suppression in migratory and adhesive properties of melanoma cells may contribute to their reduced metastatic potential.

***POMC* Gene Transfer Suppressed COX-2 Expression in Melanoma Cells.** COX-2 has been the therapeutic target of many anti-inflammatory agents for cancer therapy. To investigate whether COX-2 pathway participated in the antineoplastic and antimetastatic functions of POMC gene delivery, the COX-2 expression and PGE_2 production were analyzed in B16-F10 cells and melanoma tissue after *POMC* gene delivery. We found that *POMC* gene delivery potently reduced the COX-2 expression at mRNA and protein levels by more than 70% of that in control groups ($P < 0.001$; Fig. 5, a and b). Moreover, the release of COX-2 enzyme product, PGE_2, in Ad-POMC-treated B16-F10 cells were also decreased by 50 to 70% of that in control groups (Fig. 5c). Likewise, in tumor tissues, *POMC* gene delivery also led to a significant reduction in COX-2 protein levels compared with Ad-GFP-infected tumors (Fig. 6a). Besides, the PGE_2 level in POMC-transduced melanoma was also significantly lower than that of control groups (Fig. 6b). Histological analysis revealed a prominent COX-2 immunostaining in melanoma, but not in normal skin, indicating that COX-2 is overexpressed in B16-F10 melanoma (Fig. 6c). Above all, the COX-2 immunoreactivities were significantly lower in Ad-POMC-infected melanoma than Ad-GFP-treated ones (Fig. 6d). Therefore, *POMC* gene transfer leads to reduction in COX-2 expression and PGE_2 synthesis in B16-F10 melanoma in vitro and in vivo.

***POMC* Gene Transfer Mimicked the Antineoplastic Effect of a Selective COX-2 Inhibitor, NS-398, in B16-F10 Melanoma Cells.** To evaluate whether *POMC* gene delivery indeed acted like a COX-2 inhibitor, we made an extensive, parallel comparison on the cellular effect of *POMC* gene delivery with a selective COX-2 inhibitor. Although NS398 had no effect on cell proliferation even at doses as high as 100 μM (Fig. 7a), treatment with NS398 significantly attenuated PGE_2 production, anchorage-independent growth, and cell migration of B16-F10 cells in a dose-dependent manner (Fig. 7, b–d). Moreover, continuous administration of NS-398 prominently reduced the melanoma growth of

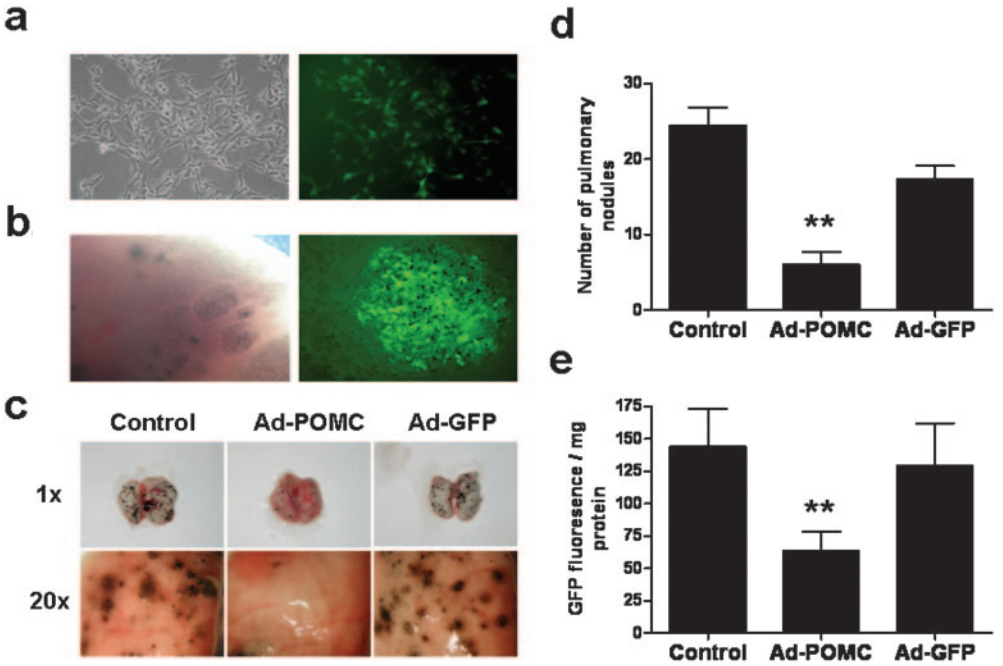

Fig. 3. Effect of *POMC* gene transfer on metastasis of melanoma cells in mice. a, characterization of GFP-expressing B16-F10 melanoma cells. The morphologies of GFP-B16-F10 cells were examined under phase contrast (left) and fluorescence microscope (right). b, the metastatic foci of GFP-B16-F10 cells in lung. After intravenous injection of GFP-B16-F10 cells for 14 days, the pulmonary foci were examined by phase contrast (left; 100×) and fluorescence microscope (right panel; 200×). c, the appearance of lung foci after intravenous injection of various B16-F10 cells for 14 days. d, quantification of metastatic event by counting lung foci number in various groups of mice. The number of lung foci were counted and expressed as mean ± S.D. after intravenous injection of different engineered B16-F10 cells into mice for 14 days ($n = 8$). **, $P < 0.001$. e, quantification of metastatic event by measuring GFP fluorescence intensity in lung extracts from mice injected with various groups of B16-F10 cells. After extraction, the GFP fluorescence intensity was determined in fluorometer and expressed mean ± S.D. arbitrary units for each group ($n = 8$). The results were representative of three independent experiments. **, $P < 0.001$.

implanted B16-F10 cells in mice (Fig. 7e). In addition, the reduced tumor volume was associated with a decreased PGE_2 content in melanoma tissues (Fig. 7f). These data indicate that the cellular influences of *POMC* gene delivery in B16-F10 cells are remarkably similar to that of COX-2 inhibitor.

***POMC* Gene Transfer Inhibited NFκB Activities in Melanoma Cells.** Because NFκB is an upstream regulator of COX-2 pathway, the effect of *POMC* gene delivery on the endogenous and stimulated NFκB activities in B16-F10 cells was investigated. *POMC* gene delivery resulted in a significant reduction in nuclear NFκB level, nuclear binding activities to NFκB motif and NFκB-driven luciferase activities by 30 to 60% of control groups (Fig. 8, left). Even in the presence of TNF-α, which markedly elevated the NFκB activities, *POMC* gene delivery still effectively repressed the TNF-α-stimulated NFκB activities in melanoma cells (Fig. 8, right). These results indicate that *POMC* gene transfer potently inhibits the NFκB activities in melanoma cells.

***POMC* Gene Transfer Inhibited the NFκB Activities, COX-2 Expression, and Melanoma Growth via α-MSH Pathway.** To identify the POMC neuropeptide(s) that contributed to inhibition of NFκB activity and PGE_2 production

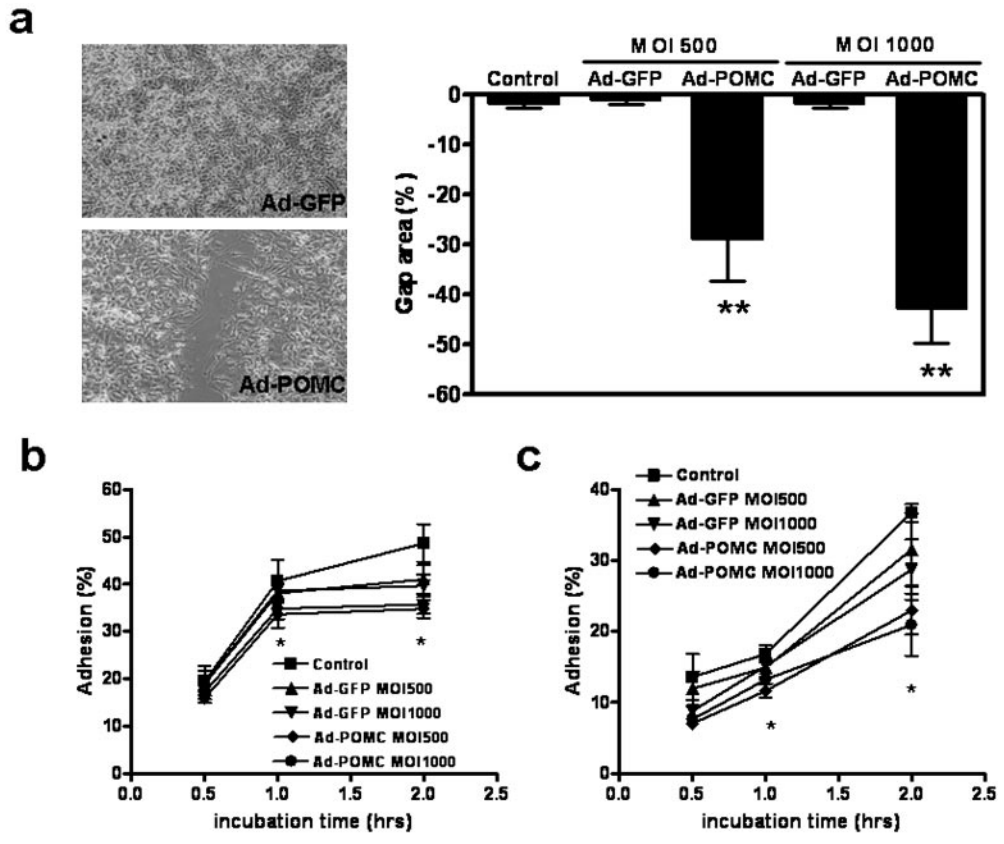

Fig. 4. Effect of *POMC* gene transfer on the motility and adhesion capability of B16-F10 melanoma cells. a, healing of scratch wounds in POMC-transduced B16-F10 cells. After infection with adenovirus vectors for 12 h, a scratch was made and the closure extent of gap was monitored by phase-contrast microscope for 24 h. Quantification of gap area in POMC-transduced B16-F10 cells at 24 h. b and c, effect of *POMC* gene transfer on the adhesion capacity of B16-F10 cells to extracellular matrix proteins. After infection with adenovirus vectors for 12 h, the binding extent of B16-F10 melanoma cells to wells coated with fibronectin (b) or laminin (c) was measured at different time courses. **, $P < 0.001$; *, $P < 0.05$.

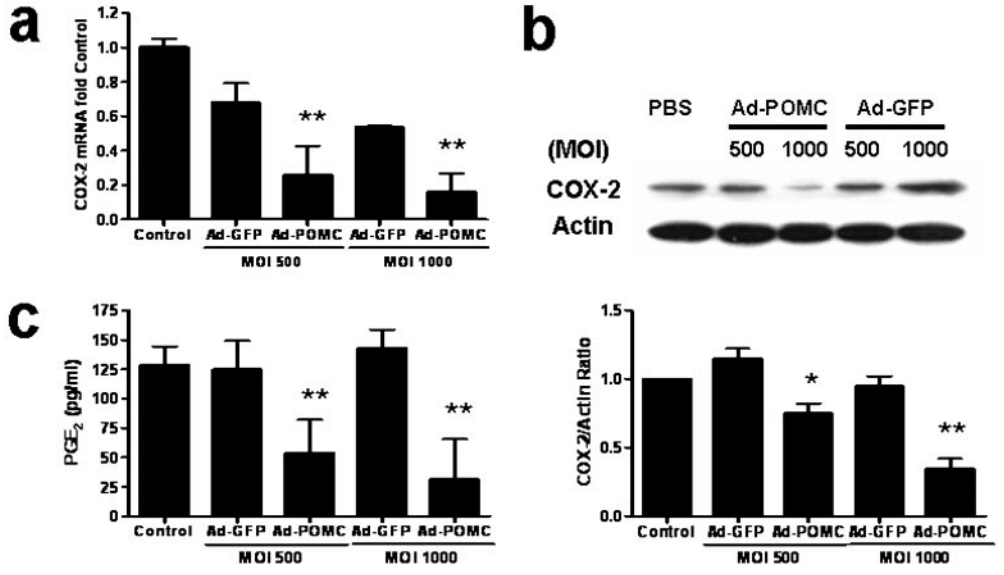

Fig. 5. Effect of *POMC* gene delivery on COX-2 expression and PGE_2 production in B16-F10 cells. a, effect of *POMC* gene delivery on COX-2 mRNA level. Real time of COX-2 mRNA in B16-F10 after *POMC* gene transfer. After infection with adenovirus vectors for 24 h, total RNA was isolated from different groups of B16-F10 cells for measurement of mRNA level by quantitative RT-PCR analysis using actin as internal control. b, effect of *POMC* gene delivery on COX-2 protein level. After infection with adenovirus vectors for 24 h, protein extract was isolated from different groups of B16-F10 cells for determination of COX-2 protein level by Western blot analysis. c, effect of *POMC* gene delivery on the PGE_2 production. After infection with adenovirus vectors for 24 h, cultured media were collected from different groups of B16-F10 cells to evaluate PGE_2 production using PGE_2 immunoassay. *, $P < 0.05$; **, $P < 0.001$.

by POMC gene delivery, B16-F10 cells were treated with various POMC peptides and assayed for NFκB-driven luciferase activities. Treatment with α-MSH, but not corticotropin or β-EP, mimicked the effect of *POMC* gene transfer in inhibition of NFκB-driven luciferase activities (Fig. 9a). Conversely, application of a selective α-MSH antagonist, GHRP-6, abolished the POMC-induced inhibition on NFκB activities (Fig. 9b) and PGE_2 release (Fig. 9d). Because protein kinase A (PKA) is a general downstream effector of melanocortin receptors including MC1R, we investigated whether H-89, a specific inhibitor of PKA, influenced the effect of *POMC* gene delivery in NFκB activities. It was found that H-89 treatment also reverted the POMC-induced inhibition of NFκB activities (Fig. 9c). Thus, α-MSH pathway plays an important role in POMC-mediated inhibition of NFκB/COX-2 pathway. To validate the involvement of α-MSH pathway, the effect of GHRP-6 on melanoma growth was investigated. Application of GHRP-6 alone had no effect on the growth of B16-F10 melanoma in mice (Fig. 9e). However, administration of GHRP-6 effectively reverted the POMC-mediated melanoma suppression in mice that the tumor size in mice implanted with Ad-POMC-infected cells increased from 2119 ± 950 to 3814 ± 1104 mm^3 after GHRP-6 administration (Fig. 9e). Together, α-MSH/MC1R pathway is critical to the POMC-mediated melanoma suppression.

Discussion

The present study demonstrates for the first time that gene delivery of POMC prohormone in melanoma cells increases the release of POMC neuropeptides, which simultaneously modulates the cytokine expression of cultured lymphocytes and attenuates the tumorigenic properties of melanoma cells, including proliferation, anchorage-independent growth, migration, and adhesion. Besides, pre- or post-treatment with POMC gene vector suppresses, rather than promotes, the growth and metastasis of melanoma in immune-competent mice. Finally, α-MSH-induced inhibition of pro-inflammatory NFκB/COX-2 pathway is involved in the antineoplastic mechanism of *POMC* gene delivery. Similar α-MSH-induced inhibition of NFκB/COX-2 activities has been reported in hypothalamus of lipopolysaccharide-treated rats via melanocortin 4 receptor (Caruso et al., 2004). Because of its potent suppression of melanoma progression in either the chemoprevention study using engineered melanoma cells or therapeutic study with established tumors, *POMC* gene delivery may constitute a novel chemoprevention or treatment modality for melanoma. Nevertheless, the optimal dose and gene delivery route for *POMC* gene delivery require further investigation. In addition, it remains to be explored whether POMC gene-based drugs could be applied to the treatment of other types of cancer.

Other than anti-inflammation, other mechanisms may participate in melanoma suppression by *POMC* gene delivery. Because of its marginal influence on cell proliferation, the anti-tumor function of POMC gene delivery is likely to be due to indirect mechanisms rather than direct cytotoxicity to melanoma cells. Because *POMC* gene transfer inhibits NFκB/COX-2 pathway, one probable mechanism is the blockade of tumor angiogenesis, because either NFκB or COX-2 pathway may regulate the expression of vascular endothelial growth factor (VEGF), an important angiogenic factor for tumor blood supply (Ditsworth and Zong, 2004; Rigas and Kashfi, 2005). In addition, a significant correlation was observed between overexpression of NFκB-p65 and vascular development in clinical melanoma specimens (Kashani-Sabet et al., 2004). Another plausible mechanism for POMC-mediated melanoma suppression is the activation of immune surveillance because the POMC-transduced cells are capable of altering the cytokines expression by lymphocytes (Fig. 1).

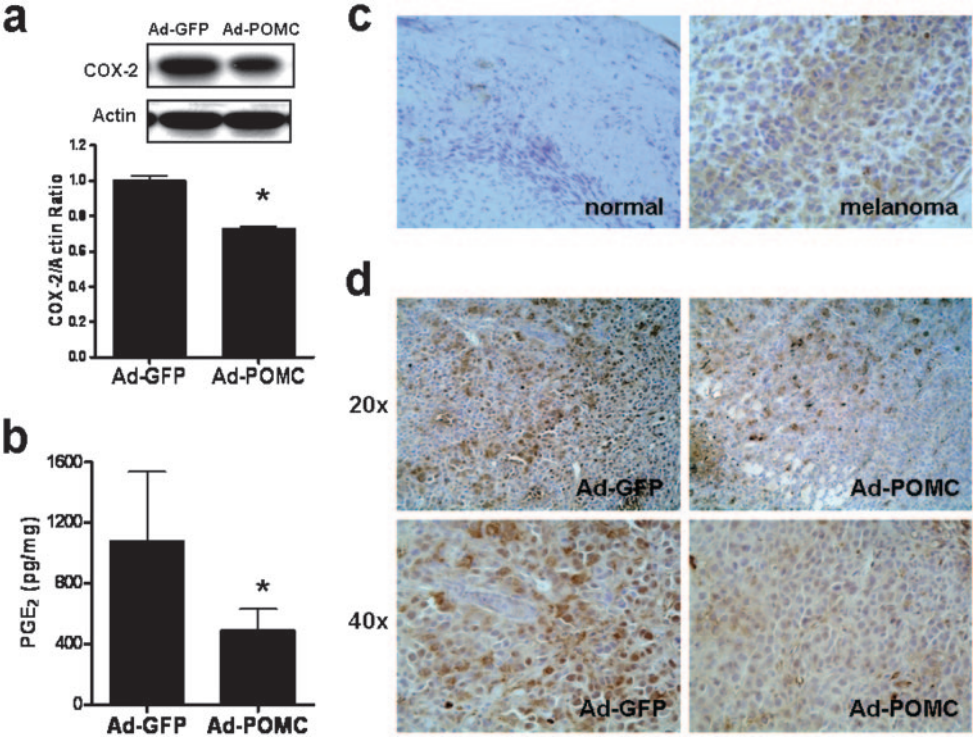

Fig. 6. Effect of *POMC* gene delivery on COX-2 expression and PGE_2 production in melanoma tissues. After implantation of various adenovirus-infected B16-F10 cells into C57BL/6 mice for 14 days, melanoma was dissected and analyzed for COX-2 expression. a, Western blot analysis of COX-2 protein level in melanoma tissues. *, $P < 0.05$. b, ELISA analysis of PGE_2 level in melanoma tissues extract. *, $P < 0.05$. c, immunohistochemical analysis of COX-2 expression in normal skin (left) and melanoma (right). d, effect of *POMC* gene delivery on COX-2 expression in melanoma tissues. Tumors derived from Ad-GFP- or Ad-POMC-infected B16-F10 cells were analyzed for COX-2 expression by immunohistochemistry. Magnification, 20× and 40×.

However, given that POMC neuropeptides are potent immunosuppressive agents, the probability of induction of systemic immunity by POMC gene delivery is relatively remote. Future studies are warranted to evaluate these mechanisms, thereby shedding light on the POMC-mediated melanoma suppression.

COX-2 and its product PGE_2 are critical to tumor growth and progression (Hla et al., 1999; Trifan and Hla, 2003). COX-2 is overexpressed in malignant melanoma and is involved in the progression and metastasis of melanoma (Denkert et al., 2001). In the present study, we provide convincing evidence that *POMC* gene delivery attenuates the COX-2 expression and PGE_2 synthesis in melanoma. How the POMC-mediated COX-2 inhibition may lead to suppression of melanoma progression and metastasis remains unclear. Recent evidence points out that COX-2 overexpression renders cancer cells resistant to apoptosis and promotes angiogenesis, invasive potential, and metastasis. Besides, melanoma inhibits the tumoricidal activity of macrophage via COX-2 expression (Duff et al., 2003). Conversely, inhibition of COX-2 could restore macrophage function in melanoma and hence maximize the antitumor activity of immune stimulants such as IFN-γ. Thus, COX-2 inhibition can suppress melanoma by induction of apoptosis and immune responses

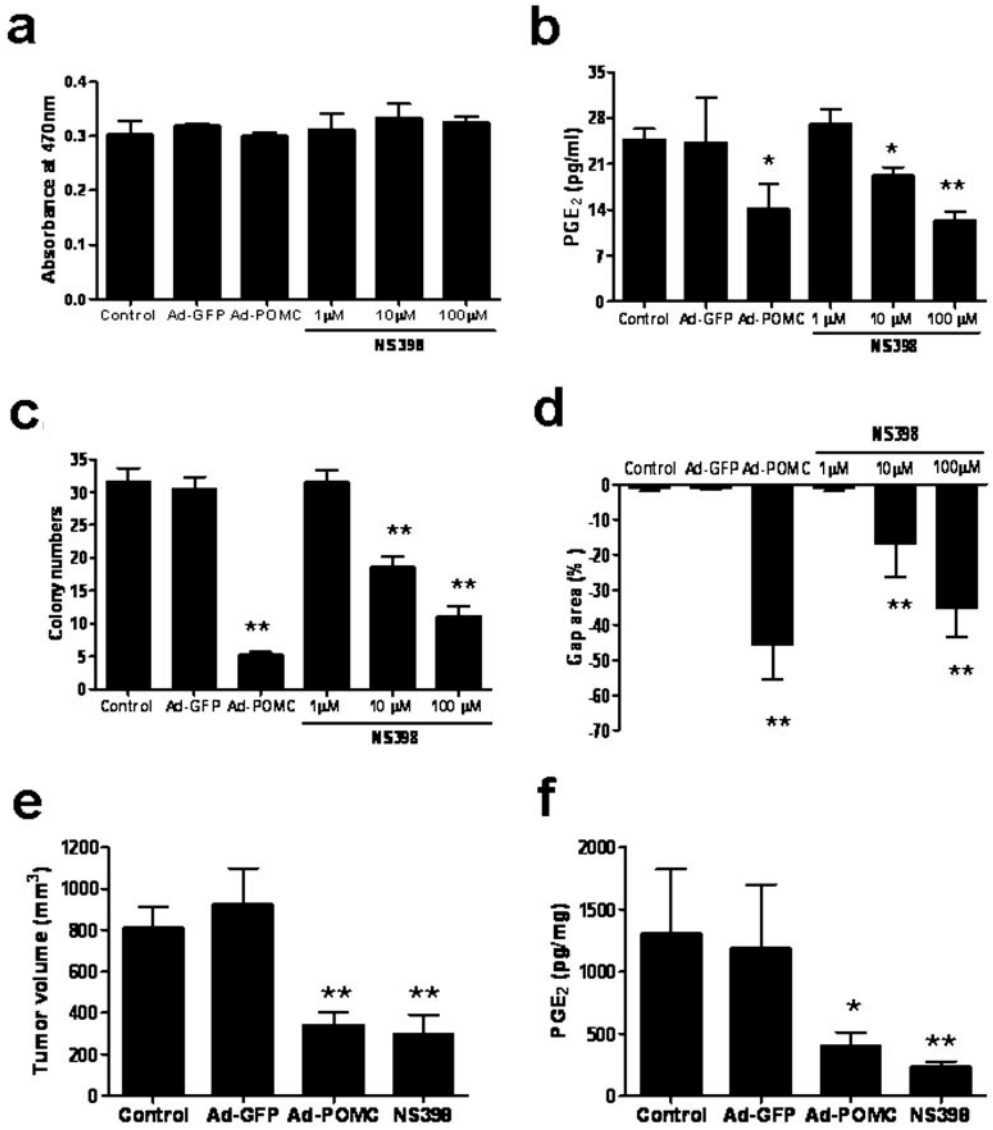

Fig. 7. Comparison of the effect of COX-2 inhibitor, NS398, and *POMC* gene transfer on the tumorigenicity of B16-F10 melanoma cells. a, cell proliferation. After treatment with NS398 (1, 10, and 100 μM) or infection with adenovirus vectors at an m.o.i. of 1000 for 24 h, the proliferation of B16-F10 melanoma cells was determined by MTT assay. b, PGE_2 production. After treatment with NS398 (1, 10, and 100 μM) or infection with adenovirus vectors at an m.o.i. of 1000 for 24 h, the culture media of B16-F10 cells were collected for analysis of PGE_2 release by ELISA. c, anchorage-independent growth. After treatment with NS398 (1, 10, and 100 μM) or infection with adenovirus vectors at an m.o.i. of 1000 for 24 h, B16-F10 cells were plated on 5% soft-agar to evaluate their colony-forming capabilities. d, cell migration. After treatment with NS398 (1, 10, and 100 μM) or infection with adenovirus vectors at an m.o.i. of 1000 for 24 h, B16-F10 cells were introduced with a scratch wound then measured for the healing extent of gap after 24 h. e, melanoma growth in mice after implantation of B16-F10 cells. After treatment with NS-398 or infection with adenovirus vectors at a m.o.i. of 1000 for 24 h, B16-F10 cells were implanted to monitor tumor growth in C57BL/6 mice ($n = 6$ per group). For NS-398 treatment, the implanted mice received daily administration of NS-398 (at a dose of 10 mg/kg) via intraperitoneal route. At day 14, the tumor volumes in different groups of mice were measured and expressed as mean cubic millimeters ± S.E.M. f, PGE_2 production in melanoma tissues. The protein extracts were isolated from melanoma tissues and analyzed for PGE_2 level by ELISA. *, $P < 0.05$; **, $P < 0.01$.

while reducing the neovascularization and invasive potential of tumor cells.

Melanoma exhibits constitutive activation of NFκB, which leads to endogenous expression of a number of factors associated with escape from apoptosis, tumorigenesis, and metastasis (Dolcet et al., 2005). On the other hand, the inhibition of NFκB has resulted in significant anti-tumor effects in melanoma (Amiri and Richmond, 2005). In the present study, POMC-mediated NFκB inhibition is mimicked by α-MSH but abolished by antagonist of MC1R or PKA, demonstrating at least the involvement of the α-MSH/MC1R/PKA signaling pathway. However, the exact mechanism underlying POMC-induced inhibition of NFκB activities remains to be delineated.

Because several POMC neuropeptides are produced in POMC-expressing melanoma cells, it is important to characterize the peptide(s) pathway that contributes to melanoma suppression by *POMC* gene delivery. The production of α-MSH by *POMC* gene transfer is postulated because the antineoplastic efficacy of α-MSH has been extensively characterized in melanoma. Treatment with α-MSH attenuates the growth of melanoma cells (Robinson and Healy, 2002), whereas the presence of wild-type MC1R is essential to the inhibitory function of α-MSH (Robinson and Healy, 2002). α-MSH was recently identified as a potential attenuating factor during progression of neuroendocrine neoplasm (Zhou et al., 2005). In the present study, we provide evidence that α-MSH treatment mimics the POMC-induced inhibition of NFκB activities in melanoma cells. Because MC1R is functional in B16-F10 cells, the antineoplastic effect of *POMC* gene delivery in melanoma supports the autocrine-inhibitory circuit for tumor suppression as in malignant mesothelioma cells (Catania et al., 2004a). In addition, application with α-MSH inhibits migration or invasiveness (Murata et al., 1999; Zhu et al., 2002; Canton et al., 2003; Eves et al., 2003; Zhu et al., 2004) and attachment to extracellular matrix protein (Robinson and Healy, 2002) in melanoma cells. Therefore, the antimetastatic effect of *POMC* gene delivery could also be attributed to α-MSH generation. Taken together, α-MSH/MC1R pathways play an essential role in the antitumor mechanism of *POMC* gene delivery in melanoma. In contrast, corticotropin or β-EP is not known for its role in skin carcinogenesis. Furthermore, treatment with naloxone did affect neither POMC-induced NFκB inhibition nor tumor suppression (data not shown), suggesting that β-EP/opioid receptors pathway is unlikely to be involved. Nevertheless, we cannot exclude the probable contribution of other POMC neuropeptides or the interaction between several POMC neuropeptides to the POMC-induced melanoma suppression.

Gene delivery of *POMC* minigene, such as α-MSH, has been applied to the treatment of inflammation in the central nervous system (Ichiyama et al., 1999), autoimmune encephalomyelitis (Yin et al., 2003), and liver failure (Wang et al., 2004). In the present study, the strategy of using the entire POMC precursor gene may be advantageous over the mini-gene approach in the following. First, the utilization of *POMC* precursor gene may be more efficient in production of POMC-derived peptides because of the preservation of the secretory and processing signals for POMC prohormone. Second, the use of natural *POMC* gene may be less immunogenic than the artificially engineered mini-genes during clinical application. Third, other than α-MSH, *POMC* gene delivery also generates other beneficiary neuropeptides such as β-EP

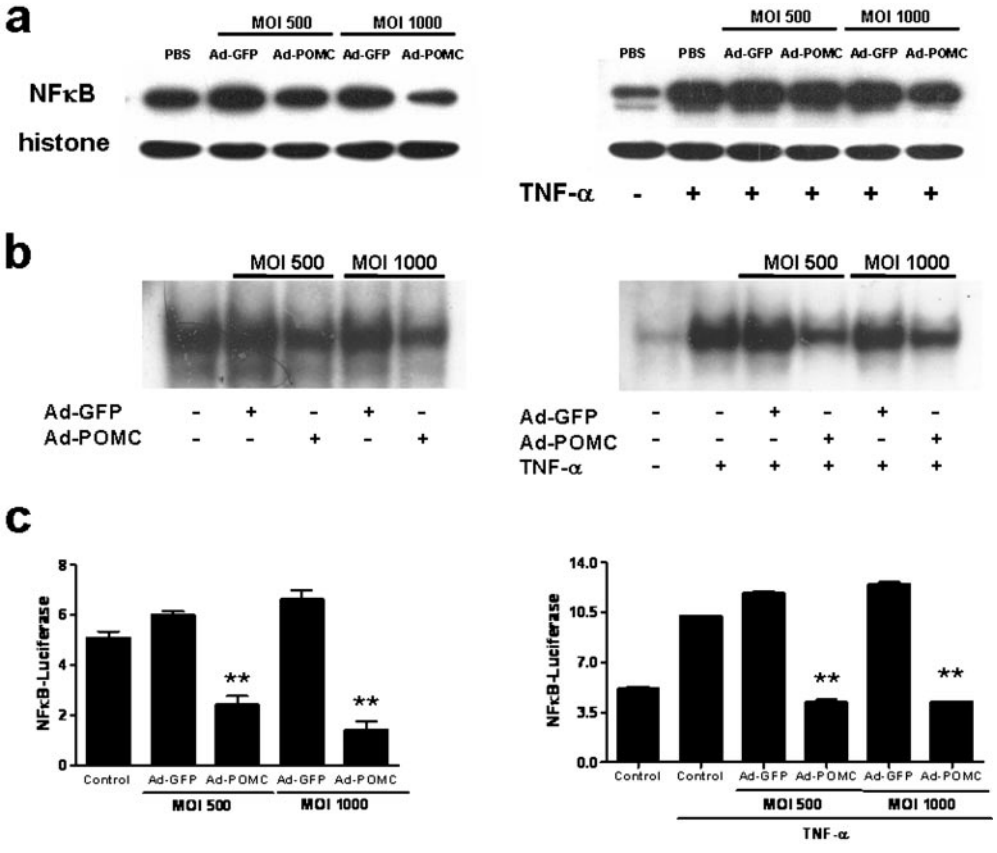

Fig. 8. Effect of *POMC* gene delivery on the NFκB activity in B16-F10 cells. The basal and stimulate NFκB activities in B16-F10 cells were measured in the absence (right) and presence (left) of TNF-α (10 ng/ml), respectively. a, Western blot analysis of NFκB expression in the nuclear extract of B16-F10 cells after POMC gene delivery. The protein expression of histone was measured as loading control for the nuclear extract. b, the electrophoretic mobility shift assay of NFκB binding activities in B16-F10 cells after *POMC* gene delivery. c, the NFκB-driven luciferase activities in B16-F10 cells after *POMC* gene delivery. **, $P < 0.001$.

in tumors or the peripheral tissues. The production of antinociceptive β-EP via *POMC* gene delivery may confer relief to the life quality of cancer patients. Previous studies indicated that transplantation of encapsulated tumor cells secreting opioid peptides such as β-EP or enkephalin provided antinociceptive effect (Gonzalez-Navarro et al., 1987; Wu et al., 1994; Saitoh et al., 1995). In addition, recent evidence indicates that *POMC* gene delivery in muscle or kidney alleviates formalin-induced pain (Lu et al., 2002) or bladder pain (Chuang et al., 2003). Hence, β-EP production in the peripheral tissues via *POMC* gene delivery may exert antinociceptive function. Because cancer pain is a devastating problem for quality of life in patients with cancer, it seems plausible that *POMC* gene delivery may inhibit neoplasm through the anti-inflammation functions but also alleviate cancer pain via the analgesic effect of β-EP.

Although in situ *POMC* gene delivery was effective and well tolerated in tumor-bearing mice, probable obstacles exist that might hinder the clinical application of *POMC* gene delivery. First, ectopic corticotropin production due to *POMC* gene transfer might result in disease states such as Cushing's syndrome (Labeur et al., 2004). Second, *POMC* gene delivery might influence various physiological parameters, such as energy balance, steroid synthesis, and behavior. Based on these aspects, future studies are warranted to shed lights on the adverse effects of *POMC* gene delivery to physiological processes, particularly steroidogenesis and native immune functions. In summary, we have demonstrated the potential of *POMC* gene delivery for treatment of melanoma and probably cancer pain. The feasibility and limitations of peripheral *POMC* gene transfer for cancer therapy remain to be elucidated.

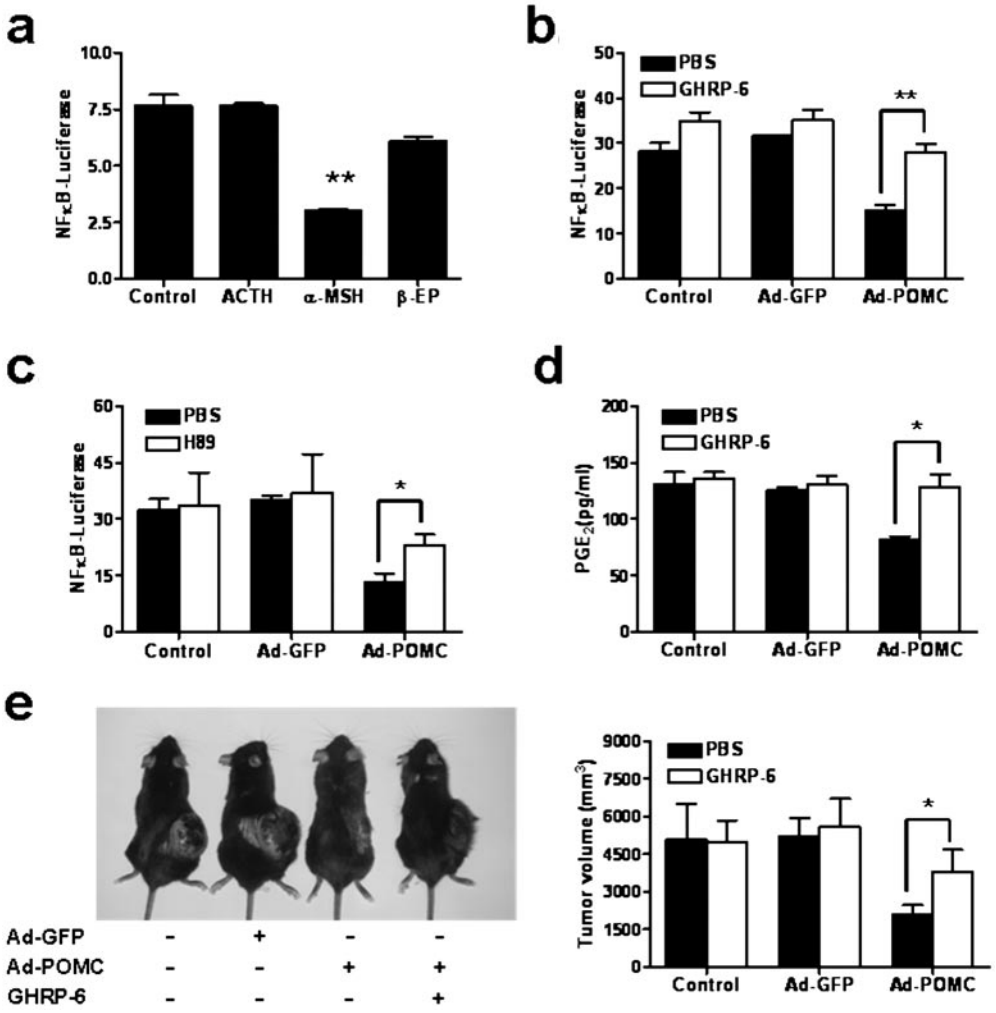

Fig. 9. Effect of α-MSH antagonist GHRP-6 on POMC-induced inhibition of NFκB activities, PGE_2 production, and melanoma growth. a, effect of POMC peptides on the NFκB-driven luciferase in B16-F10 cells. After transfection with luciferase vectors, B16-F10 cells were treated with 1 μM corticotropin, α-MSH, and β-EP, respectively, for 24 h then assayed for luciferase activities. b, effect of GHRP-6 on POMC-induced inhibition of NFκB-driven luciferase activities in B16-F10 cells. After transfection with luciferase vectors and infection with adenovirus vectors, B16-F10 cells were treated with PBS or GHRP-6 (1 μM) for 24 h then assayed for NFκB-driven luciferase activities. c, effect of H-89 on POMC-induced inhibition of NFκB-driven luciferase activities in B16-F10 cells. After transfection with luciferase vectors and infection with adenovirus vectors, B16-F10 cells were treated with PBS or H-89 (5 μM) for 24 h then assayed for NFκB-driven luciferase activities. d, effect of GHRP-6 on POMC-induced inhibition of PGE_2 production in B16-F10 cells. After infection with adenovirus vectors, B16-F10 cells were treated with PBS or GHRP-6 (1 μM) for 24 h. The culture media were collected for PGE_2 ELISA assay. e, effect of coadministration of GHRP-6 on the POMC-mediated suppression of melanoma growth in C57BL/6 mice. After infection with various adenovirus vectors, B16-F10 cells were implanted in C57BL/6 mice to monitor tumor growth ($n = 12$ per group). After implantation for 3 days, mouse was either injected with PBS ($n = 6$) or GHRP-6 (100 μg; $n = 6$). At day 21, the representative profile of melanoma growth in different groups of mice was recorded (left). The tumor size in different groups of mice were measured and expressed as mean ± S.E.M. mm^3 ($n = 6$; right). *, $P < 0.05$, **; $P < 0.001$.

References

Amiri KI and Richmond A (2005) Role of nuclear factor-kappa B in melanoma. *Cancer Metastasis Rev* **24:**301–313.

Cabot PJ, Carter L, Gaiddon C, Zhang Q, Schafer M, Loeffler JP, and Stein C (1997) Immune cell-derived beta-endorphin. Production, release and control of inflammatory pain in rats. *J Clin Investig* **100:**142–148.

Canton I, Eves PC, Szabo M, Vidal-Vanaclocha F, Sisley K, Rennie IG, Haycock JW, and MacNeil S (2003) Tumor necrosis factor alpha increases and alpha-melanocyte-stimulating hormone reduces uveal melanoma invasion through fibronectin. *J Investig Dermatol* **121:**557–563.

Caruso C, Mohn C, Karara AL, Rettori V, Watanobe H, Schioth HB, Seilicovich A, and Lasaga M (2004) Alpha-melanocyte-stimulating hormone through melanocortin-4 receptor inhibits nitric oxide synthase and cyclooxygenase expression in the hypothalamus of male rats. *Neuroendocrinology* **79:**278–286.

Catania A, Colombo G, Carlin A, Garofalo L, Gatti S, Buffa R, Carboni N, Rosso L, Santambrogio L, Cantalamessa L, et al. (2004a) Autocrine inhibitory influences of alpha-melanocyte-stimulating hormone in malignant pleural mesothelioma. *J Leukoc Biol* **75:**253–259.

Catania A, Delgado R, Airaghi L, Cutuli M, Garofalo L, Carlin A, Demitri MT, and Lipton JM (1999) alpha-MSH in systemic inflammation. Central and peripheral actions. *Ann NY Acad Sci* **885:**183–187.

Catania A, Gatti S, Colombo G, and Lipton JM (2004b) Targeting melanocortin receptors as a novel strategy to control inflammation. *Pharmacol Rev* **56:**1–29.

Chuang YC, Chou AK, Wu PC, Chiang PH, Yu TJ, Yang LC, Yoshimura N, and Chancellor MB (2003) Gene therapy for bladder pain with gene gun particle encoding pro-opiomelanocortin cDNA. *J Urol* **170:**2044–2048.

Coussens LM and Werb Z (2002) Inflammation and cancer. *Nature (Lond)* **420:**860–867.

Denkert C, Kobel M, Berger S, Siegert A, Leclere A, Trefzer U, and Hauptmann S (2001) Expression of cyclooxygenase 2 in human malignant melanoma. *Cancer Res* **61:**303–308.

Ditsworth D and Zong WX (2004) NF-kappaB: key mediator of inflammation-associated cancer. *Cancer Biol Ther* **3:**1214–1216.

Dolcet X, Llobet D, Pallares J, and Matias-Guiu X (2005) NF-kB in development and progression of human cancer. *Virchows Arch* **446:**475–482.

Duff M, Stapleton PP, Mestre JR, Maddali S, Smyth GP, Yan Z, Freeman TA, and Daly JM (2003) Cyclooxygenase-2 inhibition improves macrophage function in melanoma and increases the antineoplastic activity of interferon gamma. *Ann Surg Oncol* **10:**305–313.

Eves P, Haycock J, Layton C, Wagner M, Kemp H, Szabo M, Morandini R, Ghanem G, Garcia-Borron JC, Jimenez-Cervantes C, et al. (2003) Anti-inflammatory and anti-invasive effects of alpha-melanocyte-stimulating hormone in human melanoma cells. *Br J Cancer* **89:**2004–2015.

Ghanem G, Verstegen J, Libert A, Arnould R, and Lejeune F (1989) Alpha-melanocyte-stimulating hormone immunoreactivity in human melanoma metastases extracts. *Pigment Cell Res* **2:**519–523.

Gonzalez-Navarro A, Zimman Mansfeld H, Molinero Aparicio T, Gonzalez Hernandez MJ, Gonzalez Mate A, and Borque-Ibarra M (1987) Use of beta-endorphin in pain in cancer patients. *Vopr Onkol* **33:**26–32.

Hla T, Bishop-Bailey D, Liu CH, Schaefers HJ, and Trifan OC (1999) Cyclooxygenase-1 and -2 isoenzymes. *Int J Biochem Cell Biol* **31:**551–557.

Ichiyama T, Campbell IL, Furukawa S, Catania A, and Lipton JM (1999) Autocrine alpha-melanocyte-stimulating hormone inhibits NF-kappaB activation in human glioma. *J Neurosci Res* **58:**684–689.

Kadekaro AL, Kanto H, Kavanagh R, and Abdel-Malek ZA (2003) Significance of the melanocortin 1 receptor in regulating human melanocyte pigmentation, proliferation and survival. *Ann NY Acad Sci* **994:**359–365.

Kashani-Sabet M, Shaikh L, Miller JR 3rd, Nosrati M, Ferreira CM, Debs RJ, and Sagebiel RW (2004) NF-kappa B in the vascular progression of melanoma. *J Clin Oncol* **22:**617–623.

Labeur M, Arzt E, Stalla GK, and Paez-Pereda M (2004) New perspectives in the treatment of Cushing's syndrome. *Curr Drug Targets Immune Endocr Metabol Disord* **4:**335–342.

Lin CR, Yang LC, Lee TH, Lee CT, Huang HT, Sun WZ, and Cheng JT (2002) Electroporation-mediated pain-killer gene therapy for mononeuropathic rats. *Gene Ther* **9:**1247–1253.

Liu PY and Johansson O (1995) Immunohistochemical evidence of alpha-, beta- and gamma 3-melanocyte stimulating hormone expression in cutaneous malignant melanoma of nodular type. *J Dermatol Sci* **10:**203–212.

Lu CY, Chou AK, Wu CL, Yang CH, Chen JT, Wu PC, Lin SH, Muhammad R, and Yang LC (2002) Gene-gun particle with pro-opiomelanocortin cDNA produces analgesia against formalin-induced pain in rats. *Gene Ther* **9:**1008–1014.

Luger TA, Scholzen T, Brzoska T, Becher E, Slominski A, and Paus R (1998) Cutaneous immunomodulation and coordination of skin stress responses by alpha-melanocyte-stimulating hormone. *Ann NY Acad Sci* **840:**381–394.

Luger TA, Scholzen TE, Brzoska T, and Bohm M (2003) New insights into the functions of alpha-MSH and related peptides in the immune system. *Ann NY Acad Sci* **994:**133–140.

Manna SK and Aggarwal BB (1998) Alpha-melanocyte-stimulating hormone inhibits the nuclear transcription factor NF-kappa B activation induced by various inflammatory agents. *J Immunol* **161:**2873–2880.

Murata J, Ayukawa K, Ogasawara M, Watanabe H, and Saiki I (1999) Induction of autocrine factor inhibiting cell motility from murine B16-BL6 melanoma cells by alpha-melanocyte stimulating hormone. *Int J Cancer* **80:**889–895.

Newell-Price J, King P, and Clark AJ (2001) The CpG island promoter of the human proopiomelanocortin gene is methylated in nonexpressing normal tissue and tumors and represses expression. *Mol Endocrinol* **15:**338–348.

Nicolaou A, Estdale SE, Tsatmali M, Herrero DP, and Thody AJ (2004) Prostaglandin production by melanocytic cells and the effect of alpha-melanocyte stimulating hormone. *FEBS Lett* **570:**223–226.

Raffin-Sanson ML, de Keyzer Y, and Bertagna X (2003) Proopiomelanocortin, a polypeptide precursor with multiple functions: from physiology to pathological conditions. *Eur J Endocrinol* **149:**79–90.

Refojo D, Kovalovsky D, Young JI, Rubinstein M, Holsboer F, Reul JM, Low MJ, and Arzt E (2002) Increased splenocyte proliferative response and cytokine production in beta-endorphin-deficient mice. *J Neuroimmunol* **131:**126–134.

Rigas B and Kashfi K (2005) Cancer prevention: a new era beyond cyclooxygenase-2. *J Pharmacol Exp Ther* **314:**1–8.

Robinson SJ and Healy E (2002) Human melanocortin 1 receptor (MC1R) gene variants alter melanoma cell growth and adhesion to extracellular matrix. *Oncogene* **21:**8037–8046.

Saitoh Y, Taki T, Arita N, Ohnishi T, and Hayakawa T (1995) Analgesia induced by transplantation of encapsulated tumor cells secreting beta-endorphin. *J Neurosurg* **82:**630–634.

Schauer E, Trautinger F, Kock A, Schwarz A, Bhardwaj R, Simon M, Ansel JC, Schwarz T, and Luger TA (1994) Proopiomelanocortin-derived peptides are synthesized and released by human keratinocytes. *J Clin Investig* **93:**2258–2262.

Solomon S (1999) POMC-derived peptides and their biological action. *Ann NY Acad Sci* **885:**22–40.

Tai MH, Cheng H, Wu JP, Liu YL, Lin PR, Kuo JS, Tseng CJ, and Tzeng SF (2003) Gene transfer of glial cell line-derived neurotrophic factor promotes functional recovery following spinal cord contusion. *Exp Neurol* **183:**508–515.

Trifan OC and Hla T (2003) Cyclooxygenase-2 modulates cellular growth and promotes tumorigenesis. *J Cell Mol Med* **7:**207–222.

Wang CH, Jawan B, Lee TH, Hung KS, Chou WY, Lu CN, Liu JK, and Chen YJ (2004) Single injection of naked plasmid encoding alpha-melanocyte-stimulating hormone protects against thioacetamide-induced acute liver failure in mice. *Biochem Biophys Res Commun* **322:**153–161.

Wu HH, Wilcox GL, and McLoon SC (1994) Implantation of AtT-20 or genetically modified AtT-20/hENK cells in mouse spinal cord induced antinociception and opioid tolerance. *J Neurosci* **14:**4806–4814.

Yin P, Luby TM, Chen H, Etemad-Moghadam B, Lee D, Aziz N, Ramstedt U, and Hedley ML (2003) Generation of expression constructs that secrete bioactive alphaMSH and their use in the treatment of experimental autoimmune encephalomyelitis. *Gene Ther* **10:**348–355.

Zhong Wu X, Honke K, Long Zhang Y, Liang Zha X, and Taniguchi N (2004) Lactosylsulfatide expression in hepatocellular carcinoma cells enhances cell adhesion to vitronectin and intrahepatic metastasis in nude mice. *Int J Cancer* **110:**504–510.

Zhou Z, Flesken-Nikitin A, Levine CG, Shmidt EN, Eng JP, Nikitina EY, Spencer DM, and Nikitin AY (2005) Suppression of melanotroph carcinogenesis leads to accelerated progression of pituitary anterior lobe tumors and medullary thyroid carcinomas in Rb+/− mice. *Cancer Res* **65:**787–796.

Zhu N, Eves PC, Katerinaki E, Szabo M, Morandini R, Ghanem G, Lorigan P, MacNeil S, and Haycock JW (2002) Melanoma cell attachment, invasion and integrin expression is upregulated by tumor necrosis factor alpha and suppressed by alpha melanocyte stimulating hormone. *J Investig Dermatol* **119:**1165–1171.

Zhu N, Lalla R, Eves P, Brown TL, King A, Kemp EH, Haycock JW, and MacNeil S (2004) Melanoma cell migration is upregulated by tumour necrosis factor-alpha and suppressed by alpha-melanocyte-stimulating hormone. *Br J Cancer* **90:**1457–1463.

Address correspondence to: Dr. Ming-Hong Tai, Department of Medical Education and Research, Kaohsiung Veterans General Hospital, 386 Ta-Chung 1st Road, Kaohsiung 813, Taiwan. E-mail: mhtai@isca.vghks.gov.tw